

# APPLICATION OF THE ATTITUDE ANALYSIS OF DYNAMICS AND DISTURBANCES TOOL IN EUMETSAT'S STUDY ON THRUSTER'S ALLOCATION AND MOMENTUM MANAGEMENT FOR METEOROLOGICAL SPACECRAFTS

*Nuno Gomes Paulino<sup>(1)</sup>, Stefano Pessina<sup>(2)</sup>, João Branco<sup>(1)</sup>, Thomas Peters<sup>(1)</sup>*

<sup>(1)</sup> GMV, Isaac Newton 11 P.T.M., Tres Cantos, 28760 Madrid, Spain; Tel. +34 918072100, [npaulino@gmv.com](mailto:npaulino@gmv.com), [jbranco@gmv.com](mailto:jbranco@gmv.com), [tpeters@gmv.com](mailto:tpeters@gmv.com)

<sup>(2)</sup> EUMETSAT, Eumetsat Allee 1, Darmstadt, D-64295 Germany +49 6151-807-7  
[Stefano.Pessina@eumetsat.int](mailto:Stefano.Pessina@eumetsat.int)

## ABSTRACT

This paper presents the main features of the AADDTool - Analysis of Attitude Disturbances and Dynamics Tool – developed to analyze the impact of disturbances on the attitude dynamics, star tracker blinding, wheels momentum unloading schemes, and solar power supply, for long term missions in meteorological missions for EUMETSAT. It combines tiled 3D models for a cylindrical spacecraft (e.g. MSG) or any spacecraft with a central body and solar panels (e.g. MTG and METOP), with accurate models of space environment torques in line with ECSS standard. Foreseen continuous upgrading activity brought into AADDTool attitude dynamics propagation, spun guidance schemes, guidance programming, and the implementation of an elliptical field-of-view for the Star-Tracker analysis. Additional off-loading schemes were added for performance assessment of improved laws for wheels momentum management. Some results are presented from the most recent study with the AADDTool on the parameterization of two control safe modes for the MetOp spacecraft.

**Index Terms**—Attitude Dynamics, Environment Torques, Wheels off-loading, Star-trackers blinding, MetOp

## 1. INTRODUCTION

EUMETSAT is the “European organization for the exploitation of METeorological SATellites”. It is an independent intergovernmental organization created in 1986 to establish, maintain and exploit European systems of operational meteorological satellites. It currently operates a system of meteorological satellites, monitoring the atmosphere and ocean and land surfaces which deliver weather and climate-related satellite data, images and products – 24 hours a day, 365 days a year (see [1]). EUMETSAT currently has seven operational weather satellites. Meteosat-7,-8, 9 and 10, Metop-A, -B and Jason-2 (while Meteosat-11 is currently in an in-orbit-storage phase). Meteosat are the satellites of the geosynchronous

(GEO) fleet. There are two generations of active Meteosat satellites, Meteosat First Generation (MFG) and Meteosat Second Generation (MSG). MetOp are low-Earth orbit (LEO) polar meteorological satellites, which form the space segment component of the overall EUMETSAT Polar System (EPS). Jason-2 reliably delivers detailed oceanographic data vital to our understanding of weather forecasting and climate change monitoring.

To support both mission analyses of the future programs and the in-flight analyses for the currently flying satellites, EUMETSAT implemented a dedicated study with the objectives of modeling the dynamic loads induced by the space environment (according to ECSS Space Environment standards, ([3]) for gravity gradient, radiation pressure, air drag and magnetic field, based on prescribed orbits and attitude laws, characteristic of current and future EUMETSAT satellites, both for LEO and GEO. It assumed multiple reaction wheels control for the spacecraft, to characterize the wheel off-loading frequency/needs, based on angular momentum accumulation. This entailed a tool capable of considering the different spacecraft geometries, disturbances models and include actuation management schemes such as maximization of time between off-loading or scheduled off-loading with defined set points of the wheels speeds (or momenta). Furthermore, the tool was required to predict and analyze the blinding/occultation by Sun/Moon/Earth of instruments (such as star-trackers), together with solar-array(s) illumination.

It was from this study that the AADDTool was developed and it has been used in the past in the EUMAAD project context, to analyze the disturbances impacts on attitude of the spacecraft, star tracker blinding, momentum unloading schemes, and solar power supply. It implements an assortment of the spacecraft attitude guidance schemes, but it also allows open loop propagation of the spacecraft attitude dynamics, and their tile-by-tile analysis of the disturbances allows the user to refine the contributions and take into consideration better approximations for shadowing. The implementation relies on developed libraries implemented in Matlab/Simulink, with a modular

architecture to enable a modular design and progressive sophistication of the tool.

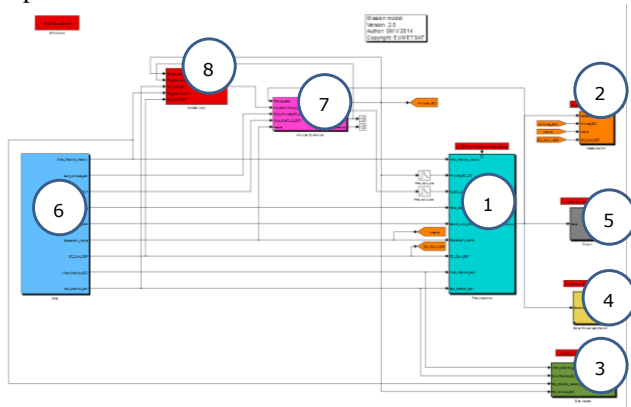


**Figure 1: Architecture of the tool, and its different components**

The tool has been applied previously in studies on LEO environment based on the currently flying EPS satellite, and GEO environment based on the future MTG satellite, focusing on characterization of disturbances and analysis of their wheels momentum management algorithms, ([2]). The most recent study was for the MetOp scenario: analyze the impact of re-tuning the default thrusters grouping numbers according to mission phases or scenarios for improvement of propellant consumption, varying the lifecycle, solar activity, and initial conditions. The study used the on-board closed loop for two operating controlled modes: Earth pointing (FAM2) and Sun pointing (PRO). For this study, the MetOp spacecraft was modeled with a tiled 3D-model using a parallelepiped for main body and rotating solar array, used to perform a tile-by-tile contribution of the disturbance torques in LEO. The impact of the closed loop settings was analyzed, and the main conclusions are summarized below in terms of overall mass consumption, and firing and attitude histories.

## 2. DESCRIPTION AND ARCHITECTURE

The tool is developed in Matlab/Simulink environment, and its architecture is based on four processes:

- Main GUI – principal interface of the user to setup the case study (spacecraft geometry, simulation, selection of attitude and disturbances)
- Config – This process parses the user input to create the spacecraft mesh, initialize the simulator data and set the input and output files. The project data saved in a global variable AADDTool accessible to all the processes in the tool.
- Mission – This process runs the analysis accordingly to the configuration set by the user. A template in Simulink is initialized and run, using the configuration

in AADDTool. The main outputs of this process are the .mat files with the outputs from the analysis.

- Display – This process is launched to post process the analysis data, generate the signal statistics, organize the data and display the figures. A folder is also created to store the project data and store the simulation and output data files.

### 2.1. Implementation

The simulation runs over Matlab using Simulink libraries and functions for the different unitary processes, propagation and integration. The configuration and setup of the mission is supported by a dedicated graphical interface for fast configuration and seamless interaction with the simulator. Post processing functions build and present the relevant batch of outputs.

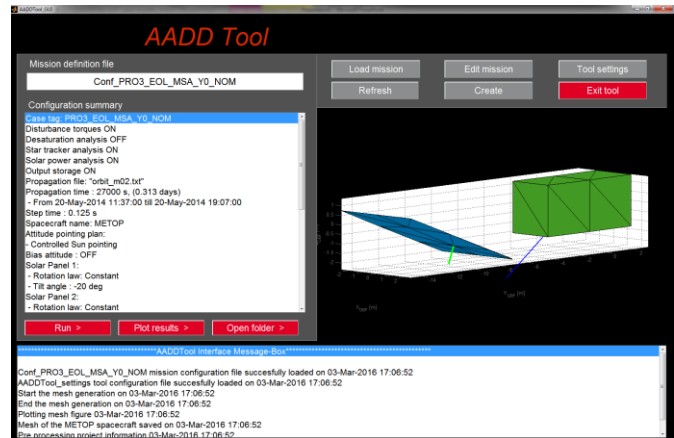


**Figure 2: AADDTool graphical user interface, for project and simulation management**

The analysis is configurable by the data extracted from an editable case study configuration file, which is prepared and generated in the configuration process. The scenario runs a Simulink template that calls and organizes the data flow among the different components of the simulation and analysis, see Figure 1:

1. Environment disturbance torques (gravity gradient, magnetic torque, aerodynamic drag, solar pressure)
2. Reaction wheels offloading analysis
3. Star tracker blinding analysis
4. Solar power estimation analysis
5. Data storage
6. Top level block that contains:
  - a. Attitude guidance law
  - b. Solar array rotation angle law
  - c. Ephemeris interpolation
  - d. Orbit history
  - e. Maneuver history

- f. Inertia update
- 7. Free dynamics computation
- 8. Metop closed loop control

The graphical interface from Figure 2 is used to manage the project and relay information to the user. Different areas of the GUI give access to a Mission definition file, allow the user to create, load and edit missions, set the general tool settings, and launch simulations and post processing. It displays the spacecraft geometry and a summary of the current configuration. The current status or errors are presented in an Interface Message box.

### 3. TOOL DESIGN

The details of the models implemented in the AADD-tool are here briefly mentioned. Full details, including algorithmic implementation, can be found in the software design document (see [5])

#### 3.1. Spacecraft geometry

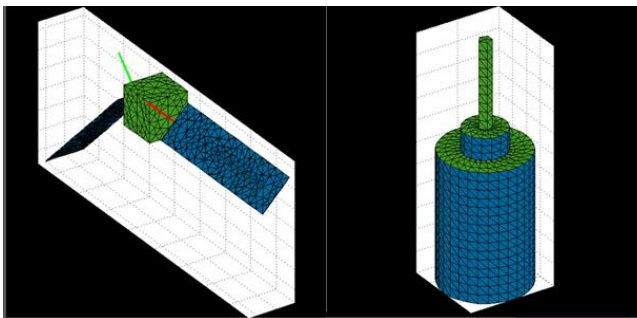


**Figure 3: 3D mesh configuration examples for MTG and MSG type spacecraft (different colors represent different optical properties)**

The spacecraft model is constituted by the central body and 1 or 2 rectangular solar panels. The central body is configured as a prism where the top and bottom areas can be different, see Figure 3 (left). These are defined in the geometric frame of the spacecraft (GBF). The solar panels are modeled as rectangular surfaces attached to the main body at a pivot point. Given the parameterization of the central body and the solar panel(s) a function automatically builds the prism and surfaces to mesh the spacecraft body. This approach simplifies the definition of the spacecraft and allows a mechanism to automatically modify the spacecraft as function of its parameters (GUI in Figure 2 shows the mesh definition for the MetOp spacecraft). The tool also allows the selection of MSG cylindrical type bodies as the one in Figure 3 (right), and the different colors indicate different optical properties of the tiles.

### 3.2 Propagation

The AADD tool performs orbit propagation, with option of pre-loading an orbit history (and interpolates with a propagator) as EME2000 time-stamped list of state vectors (position and velocity). To allow different step sizes, an interpolation is included that computes a Keplerian propagation in the instants in between samples of the orbit file. To smooth the interpolation, in fact it is carried a forward (from instant  $t_0$  to  $t_1$ ,  $t_1 > t_0$ ) and a backward interpolation (from  $t_1$  to  $t_0$ ), and both contributions are weighted by the proximity to  $t_0$  and  $t_1$ .

### 3.3 Attitude laws and dynamics

The set of implemented attitude laws comprise the needs for EUMETSAT missions, and they can be set in sequence to get a combined attitude law:

- Local orbital geocentric frame attitude (body-fixed frame with one axis pointing to Earth center and a second axis pointing towards the orbit normal)
- Local orbital geocentric frame attitude with yaw steering law (body-fixed frame with one axis pointing to Earth center and a second axis parallel to the ground-track)
- Local orbital geodetic frame attitude (body-fixed frame with one axis pointing to the local normal of the reference WGS84 ellipsoid, and a second axis pointing towards the orbit normal)
- Local orbital geodetic frame attitude with yaw steering law (body-fixed frame with one axis pointing to the local normal of the reference WGS84 ellipsoid, and a second axis parallel to the ground-track)
- Earth target pointing attitude (body frame pointing to a fixed point on the Earth surface and second axis as close as possible to the instantaneous orbital velocity or to the Earth rotation axis)
- Fixed inertial pointing attitude (for single spin stabilized spacecraft)

```
% History of attitude guidance transitions, where each line contains:
% [initial time the scheme, coding integer for the scheme]
%
Attitude_guidance_queue = [
    t           scheme
    0*24*3600   0;
    180*24*3600 2;
    360*24*3600 8;
    540*24*3600 6];
```

**Figure 4: Example of attitude law program**

These can be used as direct attitude for disturbance evaluation (assuming perfect control and navigation) or as reference for the closed loop control. Additionally, the attitude bias programming allows defining any kind of attitude manoeuvres on top of the available target pointing above, meaning the attitude law doesn't have to be static. The user has the possibility to set an attitude guidance plan,

with a queue of time of application (in seconds), and index of the attitude scheme, Figure 4. The scheme index defines the attitude law applied from that instant on:

- 0 : Local orbit Geocentric
- 1 : Local orbit Geodetic
- 2 : Earth target pointing
- 3 : Yaw steering Geocentric
- 4 : Yaw steering Geodetic
- 5 : Attitude history file
- 6 : Use Free Dynamics, without any imposed guidance attitude
- 7 : Use Spun Inertial pointing
- 8 : Use Spun Sun pointing

An important feature is the ability to integrate the free attitude dynamics, and see the impact of the disturbances. The integration law considers:

$$\mathbf{I}\dot{\boldsymbol{\omega}} = \mathbf{N}_{GG} + \mathbf{N}_D + \mathbf{N}_{MAG} + \mathbf{N}_S - \boldsymbol{\omega} \times \mathbf{I}\boldsymbol{\omega} - \dot{\mathbf{I}}\boldsymbol{\omega}$$

Where  $\mathbf{I}$  is the spacecraft's Inertia matrix in body frame,  $\dot{\mathbf{I}}$  is the variation of the spacecraft's Inertia matrix in body frame (from solar panel rotation),  $\boldsymbol{\omega}$ ,  $\dot{\boldsymbol{\omega}}$  are angular rates and angular acceleration in body frame (inputs from trajectory data),  $\mathbf{N}_D$  is the aerodynamic drag torque disturbance,  $\mathbf{N}_S$  collects the solar pressure torque disturbance,  $\mathbf{N}_{MAG}$  is the magnetic torque disturbance, and  $\mathbf{N}_{GG}$  is the gravity gradient torque vector.

### 3.4. Solar panel rotation laws

Another important feature is that the solar panels can be static, rotate with a constant rate or keep the angle to maximize the sun exposure. No dynamics is considered and discontinuities in the rotation angle are allowed, but the impact on inertia and centre of mass are taken into consideration.

### 3.5. Environment disturbances

The disturbances modelled in the AADDTool are:

- Gravity gradient torque
- Earth magnetic field torque
- Solar radiation pressure torque
- Aerodynamic drag torque

Table 1 shows the compliance of the implementation with respect to ECSS, summarising the consistency between the implementation of the effects and the ECSS standards. The main effects stated in requirements for Space Environment (gravity gradient, magnetic field, solar radiation and atmosphere) only differ to the ECSS for the wind model, not required for the tool, where a simplified co-rotating model was assumed with the atmosphere fixed to Earth.

Two other effects are taken into account, and are not specified in the ECSS: shadowing and shear stress. These two effects will impact the disturbances results since the former changes the effective area, and the latter introduces spurious tangential components to the disturbances forces (and consequent torques).

Both the sun pressure and atmospheric disturbance computation depend on the geometry of the spacecraft, and in some rotation laws, the solar panel(s) rotation changes the geometry during the simulation. Since in the tool the contribution of these effects are carried tile by tile, the mesh of tiles that constitute the surface of the spacecraft is refreshed at every simulation step; the relative position of the tiles of the solar panels is updated accordingly to the commanded solar panel angles.

**Table 1: Summary of AADDTool modeled disturbances and respective compliance with ECSS**

Effect	ECSS [3]	ACTION
Solar radiation model	Compliant with standard	-
Atmosphere model	Compliant with standard	NRLMSISE -00 model implemented (loading MSFC bulletins). JB2006 not required
Magnetic field model	Compliant with standard	IGRF-10 model implemented.
Gravity gradient torque	Not addressed in ECSS	Implemented accordingly to literature [4], without geopotential effects (Earth as point mass)
Magnetic torque	Not addressed in ECSS	Model implemented in the tool compliant with literature, see [4], and spacecraft as a single dipole.
Solar radiation pressure	Not addressed in ECSS	Model implemented in the tool compliant with literature, see [4], using 3D mesh model
Aerodynamic	Not addressed in ECSS	Model implemented in the tool compliant with literature, see [4], using 3D mesh model
Wind model	Not compliant with the standard	Not required. Simple model implemented. Atmosphere fixed with the Earth.
Shadowing	Not addressed in ECSS	Model inherited from previously implemented libraries
Shear stress	Not addressed in ECSS	Model inherited from previously implemented libraries
Planet Ephemerid	Compliant with standard	DE405 JPL ephemerid implemented.

Finally, the ephemerides computation takes the DE405 JPL databases as defined in the standard, but to speed the simulation the computation is carried using a Chebyshev polynomial fitting, with an angular error w.r.t. to the database lower than  $2 \times 10^{-6} \text{deg}$ .

It is also noted that the aerodynamic model is quite sophisticated, thanks to its heritage from dedicated studies

for the ESA (very) low-earth orbit mission GOCE (down to 250 km altitude). The aerodynamic drag acceleration is computed (according to the implemented relative wind model) using the model of Schaaf and Chambre. This is a modification of the Maxwell model introducing the accommodation coefficients, so that the pressure and shear stress are computed with a different participation of specular reflection. The introduction of an additional parameter improves the accuracy of the model. To calculate the forces upon a surface element, the momentum transfer in normal and tangential directions are evaluated.

### 3.6. Reaction wheels off-loading schemes

When reaction wheels are in place for attitude control disturbances torques acting on the spacecraft end up stored in the wheels as momentum; this needs to be transferred to the inertial system using a strategy involving the application of external torque from time to time. The AADDTool provides the libraries and models to test several desaturation schemes, either using magnetic torquers or a system of reaction thrusters (RCS). These can be used independently or together (e.g. with continuous desaturation using the magnetic field while applying periodic desaturation with the RCS).

This process is implemented with 5 sub-modules:

- A module which tracks the accumulated momentum  $\mathbf{h}$ , using the contributions during  $\Delta t$  to changes in the angular momentum  $\Delta \mathbf{h}$ , and distributes it among the wheels.
- A module that computes contributions to  $\Delta \mathbf{h}$  from dynamics and the environment, from the attitude history, and atmospheric and solar torques.
- Another module computes the contributions of  $\Delta \mathbf{h}$  from the RCS from the commands from the unloading strategy module.
- The contributions to  $\Delta \mathbf{h}$  from the magnetorquers are computed from commands from the unloading strategy manager module.
- The desaturation schemes are applied in the unloading strategy manager, which tracks the momentum and speed in each wheel as well as the total momentum and elapsed time since last unloading. It commands the direction, amount of  $\Delta \mathbf{h}$  and time for desaturation.

The configuration of the simulated scenario offers several ways to set the period or triggering for off-loading. For maximum flexibility, any of the following strategies can be set in combination.

For magnetorquer angular momentum dumping:

- Continuous unloading, where the magnetorquer is commanded to cancel (at its maximum capability) at all

times, the component of the loaded angular momentum  $\mathbf{h}$  in the direction perpendicular to the magnetic field  $\mathbf{B}$ .

- A threshold can be set so as to only activate the magnetorquers if the available controlled dipole  $\mu$  is above a minimum  $|\mu| \geq \mu_{min}$  (which will avoid using the magnetorquers when the angular momentum to unload is near the geomagnetic vector general direction)
- A threshold can be set so as to only activate the magnetorquers if any of the wheels is above a specific specified triggering threshold  $rpm_{max}$

For RCS angular momentum desaturation:

- Unload periodically where the RCS is active at a predefined rate.
- Use a time table desaturation to define specific instants for desaturation and setting using individual momentum references for each wheel associated with each instant, Figure 5.
- Define a limit for angular momentum where the RCS is activated upon a threshold and the manager will keep track of the number and instant of firings:
  - o Dump momentum upon reaching a maximum accumulated momentum threshold  $|\mathbf{h}| \geq \mathbf{h}_{max}$
  - o Dump momentum when reaching a maximum accumulated momentum or speed in any single wheel  $i$ :  

$$rpm_i \geq rpm_{max_i} \text{ or } h_i \geq h_{max_i}$$

The objective of the desaturation operation can be set to 3 different targets: dump the total momentum stored in the wheels; dump the momentum in a single wheel (the one which reached saturation); or set the wheels speeds to a specific bias speed  $m_i$ .

```

% Queue for time tabled desaturation [Nms]
%          t          hi_ref
desat_table = [ 0*24*3600  5 -5 -5 5 5;
                180*24*3600 5 -5 -5 5 5;
                360*24*3600 5 -5 -5 5 5;
                540*24*3600 5 -5 -5 5 5];

```

Figure 5: Example of wheel desaturation program

### 3.7. Instrument blinding/occultation analysis

The analysis of the Instrument blinding/occultation is of particular interest for EUMETSAT spacecraft, both for investigation of sensor blinding (as when the instrument is a Star Tracker and the Sun/Moon/Earth appears in the field of view) or potential calibration (for optical payload, the Moon is used for in-flight calibrations). This analysis is based on geometric ray tracing between the instrument and the different objects that may cause occlusion, Sun, Moon and Earth. The angle between the instrument bore-sight and the Body relative position (in spacecraft frame) is computed considering an elliptical field-of-view of the sensor. A set of

conditions is evaluated to check for blinding/occlusion of a particular Body:

- This angle is compared with the Instrument exclusion angle for the Body and the angle of the Body limb angle, to see if there is a cone intrusion (where the two cones intersect). The exclusion angle specific to the Body (user configured) determines how much can the Body cross into the visibility cone without causing blinding. Separate exclusion angles can be set for the Sun, Moon and Earth.
- The Phase of the Body (for Moon and Earth only) is also compared to thresholds above which the illumination becomes relevant for the blinding decision.
- The final condition is if the Body isn't behind the Earth (for Moon and Sun only).

If all conditions are fulfilled, then this Body is causing an Instrument blinding. The blinding is flagged every time a blinding/occultation of one of the celestial bodies occurs: Moon, Earth, or Sun blinding.

It is assumed that the Instrument cone is not blinded by elements of the spacecraft itself and that the Instrument location is approximated by the Spacecraft reference frame origin. The tool foresees the configuration of up to 3 star-trackers and analyses obtainable by this functionality are applicable for any sensor with conical field of view (with circular or elliptical section).

### 3.8 Solar power estimation

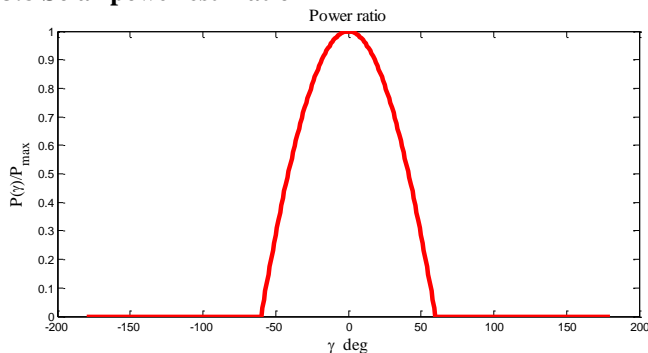


**Figure 6: Function between ratio of available power and solar incidence angle**

The power supplied by the solar arrays can be estimated from the solar radiation angle on the panels, and the same information used to evaluate the solar exposure to solar pressure can be used to estimate the power supply where the maximum power will be available when the sun line is normal to the array. A trigonometric relationship can be found between the sun incidence angle  $\gamma$  and the power available:  $P_{available} = area * \cos\gamma * P_{max}$ . Typically this holds up to 60 degrees, after which it is no longer representative. When the incidence starts getting parallel to the solar array surface, effects like finite thickness of the

cells and specular reflection from the cover glass surface, break this relationship, leading to the selected function of power ratio depicted in Figure 6, which replaces the  $\cos\gamma$  in the expression above.

The incidence angle of the solar panels and illuminated surface is retrieved from the shadowing analysis and solar pressure analysis. In the sun pressure computation, the illumination and incidence angle is evaluated for each one of the tiles that compose the spacecraft mesh and the incidence angle is taken as the mean only for the illuminated tiles. This approach also allows the use of the shadowing analysis (to remove shadowed areas of the solar panels) and provides a better estimation of the illuminated area for power supply computation.

### 3.9 MetOp closed loop

The most recent study with the AADDTool was in the MetOp scenario. There are 2 different AOCS safe modes for MetOp, PRO and FAM2, both based on exclusive control by means of thrusters. The control involved is a pulse frequency modulator, dedicated to the thrusters' triggering management. The required torque is achieved by modulating the inhibition duration following a period of constant actuation. The required torque is computed based on angular de-pointing (2 angles) with respect to either the Sun for the PRO-mode (the true "safe mode" for the spacecraft, involving a full-redundant hardware) or the Earth for the FAM2-mode (that is the final step and waiting mode with safe Earth pointing, after AOCS acquisition sequence, from random tumbling and rate reduction; this mode is used from the very first acquisition after separation with launcher, and in case of failures during the mission).

A closed loop module was developed and validated with flight data, using for sensing:

- A simplified geometric body sensor to supplies the Sun or Earth direction in sensor frame
- A "perfect" gyro to supplies angular velocity

It then performs:

- the deviations computation to supply the control the error signals
- the desired torque computation, using the control law

And for actuation modeling it performs:

- pulse modulation, accordingly to the algorithm on-board to generate the pulses issued to the thrusters
- a thruster model, based on performance laws depending on reference pressures and specific impulse
- and computes applied torque, meaning the effective torque passed to the body dynamics

The measurement of the angles merely obtains the rotation between the body direction  $p_t$  and the reference axis  $p_r$

given by:  $R_Y(\Theta_{MY})R_X(\Theta_{MX})p_r = p_t$ . As the error is cancelled, null error implicates tracking of the reference:

$$\Theta_{MY} \rightarrow 0, \Theta_{MX} \rightarrow 0 \Rightarrow p_t \rightarrow p_r$$

The estimation of attitude and attitude rates follow the onboard algorithm presented in [6] module M342111.

The implementation of the control law, which converts the error angles into desired torque at a rate of 8 Hz, is taken from pseudo-code from [6] module M3433 and parameterized with a set of integer gains from [7].

The pulse modulation is kept as on-board accordingly to pulse construction in [6] module M352111 and module M352112. The configuration for the modulation is also taken from [7].

The thruster models consider reference values for the specific impulse ( $ISP_{ref}$ ), pressure ( $P_{ref}$ ) and thrust force ( $F_{ref}$ ), at different times of the spacecraft life cycle begin of life (BOL), mid-life (MOL) and end of life (EOL):

$$F_{thrust} = f(F_{ref}, P_{ref})$$

$$ISP = g(ISP_{ref}, P_{ref})$$

Especially relevant for analysis is the mass of propellant consumed given a profile of firings. The mass used is updated at every sampling based on the thrusters levels  $F_i$  and respective specific impulse  $P_i$ , through:

$$m_i(k) = \frac{F_i(k)}{ISP_i * g_0} \Delta t_i(k) + m_i(k-1)$$

Finally, to compute the force and torque applied to the dynamics, individual forces applied by each torque are combined using their location and direction, to obtain the resulting torque in spacecraft frame.

#### 4. TOOL VALIDATION

A strong effort has been put in step-by-step validation during the development of the tool, with libraries unitary verification (in individual test setups with reference data), followed by a validation at system level against independent tools or available flight/sensor data. The independent software tools for validation include STK, NAPEOS, Simulink Aerospace Blockset, while flight data are taken from the EUMETSAT operated satellites, mainly MSG and MetOp. The test campaign up to the latest version of the tool went through a total of 58 unit test (verification of single functionalities of the tool) and 17 system tests, combining sub-sets or the entire modules of the simulation.

Some results on the system validation show an excellent agreement between the wheels speed simulated with the AADDTool and the values from actual MetOp in-flight, Figure 7. This test validated the attitude guidance (geodetic pointing with yaw steering), the disturbance models (all effects considered), the wheel loading algorithm, and the desaturation scheme with continuous off-loading using exclusively magnetorquers. The reference data originates

directly from MetOp's metrology, reporting the wheel speed evolution in-flight while continuous that operates in similar conditions. Results could be even further improved with fine tuning of the assumed simulation model for the spacecraft residual dipole (in magnitude and direction) which is not known on-ground for MetOp, and also modifying the default thermo-optical properties, to take into account aging of materials ([2]).

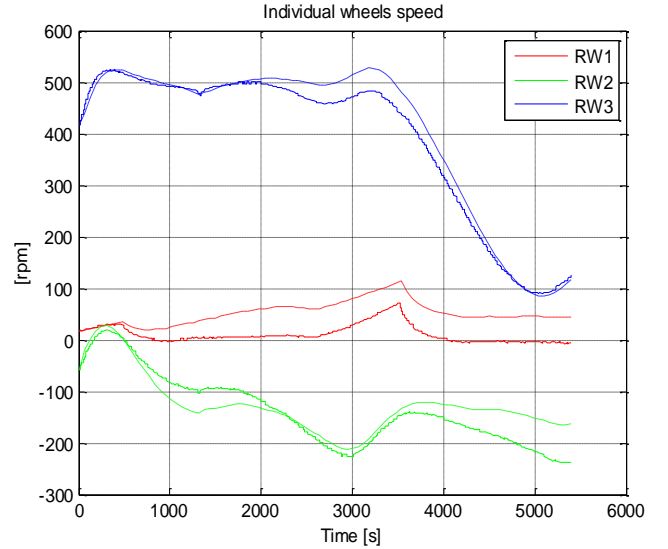


**Figure 7: Validation of simulated reaction wheels speed vs. MetOp telemetry flight data**

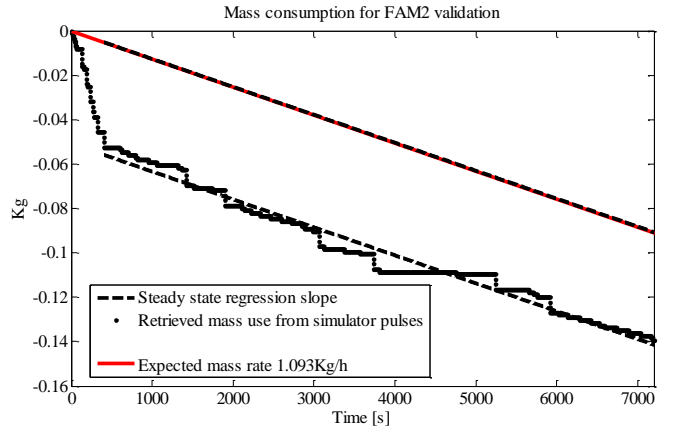


**Figure 8: Mass consumption for FAM2 during the validation test**

The implementation of the closed loop modes for MetOp flight software was validated with the trend on thrust use, respective mass consumption, and deviation in pointing and rate errors, by comparing the ones predicted by the tool against reference data: FAM2 validation data was taken from actual LEOP telemetry, that is the only time in the mission when the mode was used in flight; for PRO, the data

comes from on-ground simulated telemetry from the operational simulator (as no flight data were available) which is very representative for the AOCS, emulating the actual flight software with simplified environment and spacecraft hardware models.

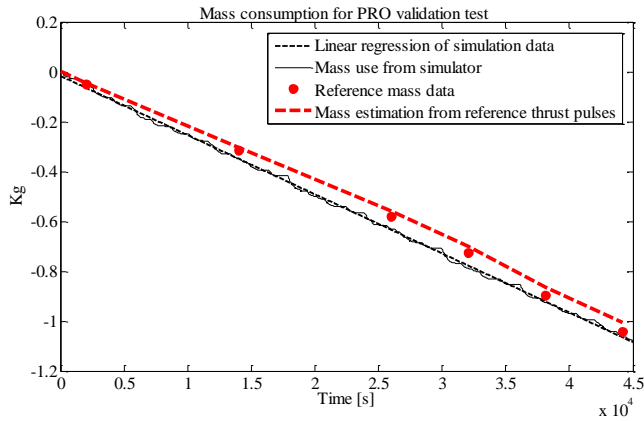


**Figure 9: Comparison of mass consumption for PRO mode during the validation test with mass consumption estimated from reference data**

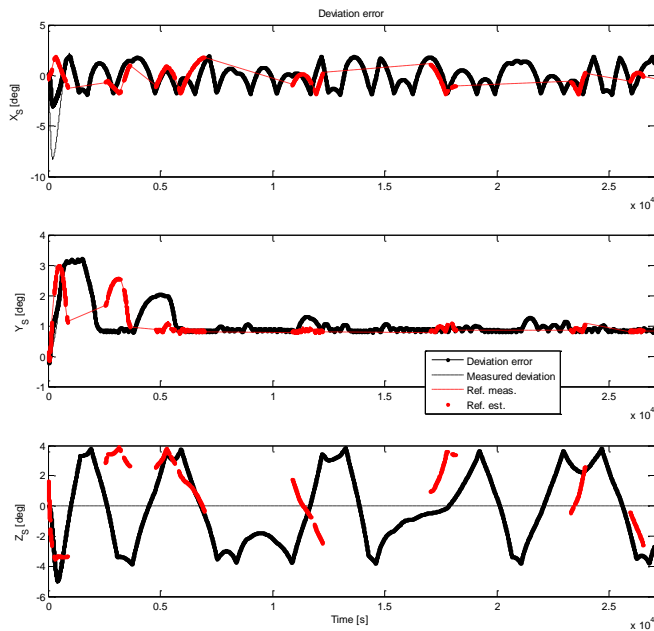


**Figure 10: Deviation pointing error in FAM2 (black) vs telemetry when available (red).**

For both of Earth (FAM2) and Sun (PRO) pointing modes, the simulated mass usage shows the same trends as the expected or reference data consumption, Figure 8 and Figure 9. In the FAM2 case there is a correction of an initial attitude error causing an initial higher consumption of mass. However, once it reaches around the reference attitude (as in

the reference data), the trend of mass use from simulation matches the expected reference slope.

More strikingly in FAM2 mode in Figure 10, the behaviour of the pointing deviation error from the AADDTool (black) mimics behaviour of the reference data segments (red) even if misplaced in time, pointing to an overall similar dynamic behaviour of the closed loop and disturbances.

## 5. RESULTS FOR METOP ANALYSIS OF CONTROL PARAMETERISATION

For this study, the MetOp spacecraft was modeled with a tiled 3D-model using a parallelepiped for main body and rotating solar array, used to perform a tile-by-tile contribution of the disturbance torques in LEO.

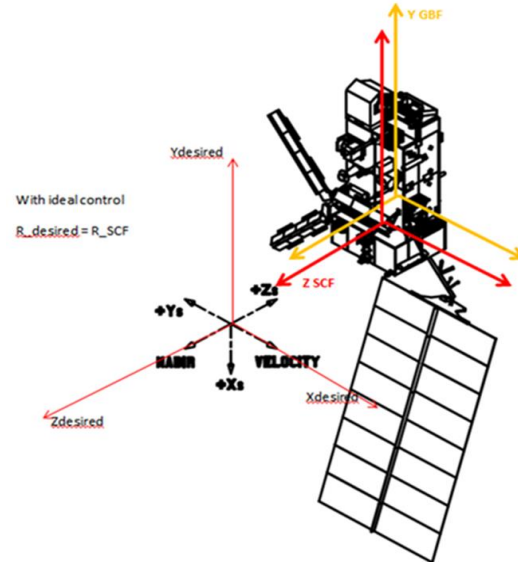


**Figure 11: MetOp spacecraft and frames: “SCF” and “GBF” frames (defined in AADDTool), and “S” frame specific to the METOP spacecraft (most of the closed loop parameters are set in this frame)**

The MetOp scenario involves a LEO orbit of about 100 minute period, with a large central body with rotating large Solar panel (Figure 11), and in this particular case two operating modes: FAM2 for Earth pointing and PRO for Sun pointing. The modes are similar, but for PRO some parameterization is simplified, with null roll bias angle and guiding rates, no presence of lag filter in control law, and fixed solar panel (while in FAM2 it follows the exposition maximization law). Also for PRO,  $Z_S$  is not estimated nor controlled. The coefficients for thruster’s parameterization are taken from [7], and three moments in the lifecycle are considered (BOL, MOL, and EOL) which vary in mass, inertia, center of mass, thruster pressure, and parameterization of the control.



The objective was to analyze the impact of re-tuning some of the control default parameterization for different life cycles, and search for improvement of propellant consumption. During FAM2 and PRO mode, the required torque is achieved with thrusters by modulating the inhibition duration following a period of constant actuation. The commanded inhibition period is computed as a function of the pulse grouping number, which varies during the whole satellite life (as a function of external disturbing torques and available thruster torques). In addition, Roll bias angle can be used in FAM2 (up to 3 degrees) to reduce hydrazine consumption due to gradient gravity torques ([6]). Both of these parameters impact directly the number of activations and mass consumption. Finally, it was also checked the impact for the level of Sun activity.

### 5.1. FAM2 mode results

Table 2 summarizes the different variations of the parameterization or scenario w.r.t. to nominal. Case FAM2-1 is to be used as reference for BOL cases, while FAM2-2 is the reference for MOL cases. The objective is to check the sensitivity to mass (1 vs 2 vs 3), bias in roll attitude (1 vs 6 and 2 vs 7), and the “grouping” number in Y-axis (1 vs 4 vs 8, 2 vs 5 vs 9) . The main criteria to be analyzed are the mass consumption (based on ISP and opening times) and stability.

**Table 2: Tested variations to the FAM2 baseline parameterization**

Case Tag	Life cycle	Solar activity	Roll bias [deg]	Pulse grouping
FAM2-1	BOL	Med.	2.0	Nominal BOL
FAM2-2	MOL	Med.	2.0	Nominal MOL
FAM2-3	EOL	Med.	2.0	Nominal EOL
FAM2-4	BOL	Med.	2.0	Nom. BOL +1 (in Y)
FAM2-5	MOL	Med.	2.0	Nom. MOL +2 (in Y)
FAM2-6	BOL	Med.	3.0	Nom. BOL
FAM2-7	MOL	Med.	3.0	Nom. MOL
FAM2-8	BOL	Med.	3.0	Nom. BOL +1 (in Y)
FAM2-9	MOL	Med.	3.0	Nom. MOL +2 (in Y)

Table 3 summarizes the consumptions for the different cases. Mass consumption slightly improved for BOL by increasing the grouping number Y+1: FAM2-4 vs FAM2-1. It was inconclusive if the bias difference results in a better consumption rate for BOL: FAM2-6 vs FAM2-1 and FAM2-8 vs FAM2-4. In the latter case, the use of a 3 deg bias seems to counter act the gains of increasing the grouping number. For MOL the 3 deg bias has a significant

impact singling out case FAM2-7. The 3 deg bias combined with Y+2 (FAM2-9) seems to cancel the benefits of the bias. Comparing the consumption rates for MOL and comparing them w.r.t. to the nominal setup, by far the best consumption rate is to increase the roll bias angle to 3 deg (a 37.76% reduction): FAM2-7 vs FAM2-2. This is in discord with the results for BOL, showing that in different life cycles, the best strategy modifications can be different. Comparing the nominal setup consumption rates, it is clear that the mass consumption decreases with time, despite a higher thrust use. The difference is more significant from BOL to the other life cycles.

**Table 3: Total consumption for the FAM2 test cases, and variations w.r.t. to the baseline**

Case	Life Cycle	Kg/day	% w.r.t. FAM21
FAM2-1	BOL	-0.8859	100.0000
FAM2-4	BOL	-0.7922	89.4200
FAM2-6	BOL	-0.8286	93.5388
FAM2-8	BOL	-0.8415	94.9918
Case		Kg/day	% w.r.t. FAM22
FAM2-2	MOL	-0.7766	100.0000
FAM2-5	MOL	-0.7368	94.8779
FAM2-7	MOL	-0.4833	62.2352
FAM2-9	MOL	-0.7826	100.7833
Case		Kg/day	% w.r.t. FAM21
FAM2-1	BOL	-0.8859	100.0000
FAM2-2	MOL	-0.7766	87.6589
FAM2-3	EOL	-0.7298	82.3794

### 5.2. PRO mode results

Table 4 summarizes the different variations tested w.r.t. to nominal and respective consumption rates. Case PRO-2 is to be used for comparison with all remaining cases. Tests PRO-2, 1, 3 check for sensitivity to mass changes due to life cycle, while Case PRO-2, 4 compare for different levels of solar activity. Case PRO-2, 5, 6 check the sensitivity to variations in the pulse grouping number for Y-axis. In PRO, the  $Z_S$  axis is not measured or control, and Case PRO-2, 7,8,9 test the impact of the initial attitude, initialized at 90 deg steps around sun direction, Figure 12. The outputs/criteria to be analyzed are again stability and mass consumption.

Effects of the different configurations are visible in the resulting consumption rates, with PRO-8 and PRO-9 to appear more beneficial than the rest. Regarding the lifecycle, MOL (PRO-2) has a consumption marginally higher EOL, but almost 4% more than BOL (PRO-1). The presence of a higher solar activity increases the consumption

rate in less than 1% (PRO-2 vs PRO-4), which is expected given the impact of drag is less than other disturbances such as gravity gradient. Modifying the grouping number has a slight impact on the consumption rate. Increasing Y+1 increases the rate in less the 0.2% (PRO-5 vs PRO-2). Decreasing the grouping number decreases the consumption in more than 2% (PRO-6 vs PRO-2).

**Table 4: Tested variations to the PRO baseline parameterization**

Case Tag	Life cycle	Solar activity	Yaw rotation [deg]	Pulse grouping	Kg/day	% w.r.t. PRO2
PRO-1	BOL	Med.	0	Nominal	-2.0756	96.0863
PRO-2	MOL	Med.	0	Nominal	-2.1601	100.0000
PRO-3	EOL	Med.	0	Nominal	-2.1593	99.9611
PRO-4	MOL	High	0	Nominal	-2.1794	100.8894
PRO-5	MOL	Med.	0	Nom.+1 (Y only)	-2.1643	100.1918
PRO-6	MOL	Med.	0	Nom.-1 (Y only)	-2.1090	97.6341
PRO-7	MOL	Med.	90	Nominal	-2.1712	100.5119
PRO-8	MOL	Med.	-90	Nominal	-1.9466	90.1162
PRO-9	MOL	Med.	180	Nominal	-1.8236	84.4207

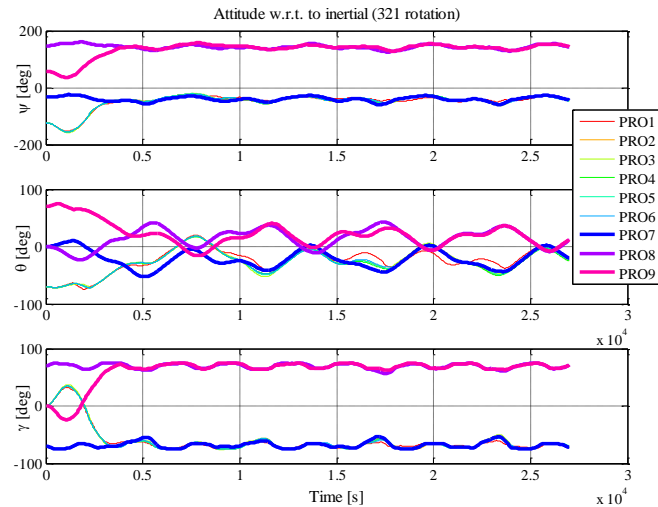


**Figure 12: Attitude history of the spacecraft, with highlighted in bold the cases where the initial conditions are rotated around the Sun direction (w.r.t. to PRO-2)**

The initial orientation of the spacecraft has the most impact on the consumption. Since the angle around the Sun direction ( $Z_S$  axis) is not controlled in this mode, a reorientation occurs at the beginning of all simulations towards 2 stable orientations, Figure 12:  $\{\psi \approx 140, \gamma \approx 70\} deg$  (PRO-8) vs  $\{\psi \approx -40, \gamma \approx -70\} deg$  (PRO-7). These stable reorientations seem to be due to dynamics,

where the former is beneficial in terms of consumption reducing the mass rate in 10 to 15%. The results point out that there seems to be a preferred rotation about  $Z_S$  for which the consumption can be minimized, however the entry point for this mode control after rate reduction is random and cannot be controlled.

## 6. CONCLUSIONS

The AADDTool's structure and philosophy has been presented, with an overview of its implementation and pointing out its main functionalities. Moreover, since its conception the AADDTool was thought to be a modular and flexible tool prepared for the continuous integration and tests of new features: already with a validated and proven version, the tool has gain new features which were presented here, along with a sample of the results obtained in the latest study carried with this tool. The impact of the closed loop settings for MetOp was analyzed varying the lifecycle, solar activity, and initial conditions, and the main conclusions are summarized in terms of overall mass consumption, and firing and attitude histories. It provided a case study to employ and demonstrate successfully the MetOp OBSW algorithms integrated in the AADDTool and it pushed forward the confidence in the tool into the analysis of closed loop systems and potential in-flight tuning of AOCS parameters for overall propellant optimization.

## 8. REFERENCES

- [1] EUMETSAT web-site [www.eumetsat.int](http://www.eumetsat.int)
- [2] Pessina S., Gomes Paulino N.M., De Juana J.M., Righetti P., "Eumetsat Study For Attitude Dynamics And Disturbances In Leo And Geo Environment", Poster session, 24th International Symposium On Space Flight Dynamics, Maryland, USA, May 2014
- [3] ECSS Space engineering Space environment, ECSS-E-ST-10-04C, 15/11/2008
- [4] Spacecraft Attitude Determination and Control, James Richard Wertz, Springer
- [5] AADD software design document GMV-EUM-AADD-SDD, Issue 2.0, Date 7/1/2015
- [6] Technical Specification of the METOP central flight software MO.RS.MMT.SV.0010 Issue 4 Rev 3 15/4/2011
- [7] METOP Numerical Values Review AOCS Data Justifications MO.NT.MMT.SV.00196 Issue 8 Rev 0 26/1/2012